Article

TGF-beta Modulates the Integrity of the Blood Brain Barrier in Vitro, and is Associated with Metabolic Alterations in Pericytes

Leonie Schumacher [1], Rédouane Slimani [2,3], Laimdota Zizmare [4], Jakob Ehlers [1], Felix Kleine Borgmann [2,3], Julia C. Fitzgerald [5], Petra Fallier-Becker [6], Anja Beckmann [7], Alexander Grissmer [7], Carola Meier [7], Ali El-Ayoubi [1], Kavi Devraj [8,9], Michel Mittelbronn [2,3,10-13], Christoph Trautwein [4*], Ulrike Naumann [1*]

[1]Molecular Neurooncology, Department of Vascular Neurology, Hertie Institute for Clinical Brain Research and Center of Neurology, University of Tübingen, Germany
[2]Department of Cancer Research (DOCR), Luxembourg Institute of Health (LIH), Luxembourg
[3]Luxembourg Centre of Neuropathology (LCNP), Luxembourg
[4]Werner Siemens Imaging Center, Department of Preclinical Imaging and Radiopharmacy, University of Tübingen, University Hospital Tübingen, Germany
[5]Mitochondrial Biology of Parkinson's Disease, Department of Neurodegenerative Diseases, Hertie Institute for Clinical Brain Research and Center of Neurology, University of Tübingen, Germany
[6]Institute for Pathology and Neuropathology, University of Tübingen, Germany
[7]Department of Anatomy and Cell Biology, Saarland University, Homburg, Germany
[8]German Cancer Consortium (DKTK), Heidelberg, Germany
[9]Edinger Institute (Neurological Institute), Goethe University Hospital, Frankfurt/Main, Germany
[10]Luxembourg Centre for Systems Biomedicine (LCSB), University of Luxembourg, Luxembourg
[11]Department of Life Sciences and Medicine (DLSM), University of Luxembourg, Esch-sur-Alzette, Luxembourg
[12]Faculty of Science, Technology and Medicine (FSTM), University of Luxembourg, Esch-sur-Alzette, Luxembourg
[13]National Center of Pathology (NCP), Laboratoire Nationale de Santé (LNS), Luxembourg
* Correspondence: Ulrike Naumann, Email: ulrike.naumann@uni-tuebingen.de; Christoph Trautwein: Email: christoph.trautwein@med.uni-tuebingen.de

Abstract: The blood-brain barrier (BBB) is a selectively permeable boundary that separates the circulating blood from the extracellular fluid of the brain and is an essential component for brain homeostasis. In glioblastoma (GBM), the BBB of peritumoral vessels is often disrupted. Pericytes, being important to maintain the BBB integrity, can be functionally modified by GBM cells which induce proliferation and cell motility via the TGF-β-mediated induction of central epithelial to mesenchymal transition (EMT) factors. We demonstrate that pericytes strengthen the integrity of the BBB in primary endothelial cell/pericyte co-cultures as an *in vitro* BBB model, using TEER measurement of the barrier integrity. In contrast, this effect was abrogated by TGF-β or conditioned medium from TGF-β secreting GBM cells, leading to the disruption of a so far intact and tight BBB. TGF-β notably changed the metabolic behavior of pericytes, by shutting down the TCA cycle, driving energy generation from oxidative phosphorylation towards glycolysis, and by modulating pathways that are necessary for biosynthesis of molecules used for proliferation and cell division. Combined metabolomic and transcriptomic analyses further underscored that the observed functional and metabolic changes of TGF-β-treated pericytes are closely connected with their role as important supporting cells during angiogenic processes.

Keywords: Glioblastoma; blood brain barrier; transforming growth factor beta; metabolomics

1. Introduction

The blood–brain barrier (BBB) is a highly selective barrier that prevents the non-selective transport of molecules from the blood into fluids of the central nervous system (CNS). It is formed by endothelial cells (EC) building the capillary walls, by pericytes that are embedded in the basal membrane and is supported by astrocytes, the latter enrobing the capillary structure with their end feet. An intact BBB is highly important to maintain

 doi:10.20944/preprints202212.0342.v1

homeostasis in the central nervous system (CNS) since it allows the transport of molecules into the brain that are essential for its function. On the other hand, it protects the brain towards pathogens. However, the BBB is also a major obstacle for the transport of drugs into brain tumors, at least in the infiltration zone of these tumors and for those tumor cells that deeply infiltrated the healthy brain and that are located far away from the original tumor (for review see [1]). In neurological diseases, especially in glioblastoma (GBM), the most malignant brain tumor of adults, the BBB in and around the tumor core is leaky, leading to peritumoral edema and thus, to neurological deficits and a poor clinical outcome [2]. GBM induced cerebral edema is currently treated with the corticosteroid dexamethasone (DEX) due to its ability to decrease BBB permeability. However, DEX, being an immunosuppressive drug, may be detrimental to immunotherapy in GBM patients [3]. In this regard, it is of central importance to understand why in GBM the BBB becomes disrupted and how this leakiness can be reduced or even prevented to avoid the use of corticosteroids.

Pericytes are mural cells adjacent to endothelial cells, wrapping around blood vessels. In the CNS, pericytes are necessary for the formation and regulation of the BBB. Under pathological conditions, such as in GBM, pericytes often undergo a functional change (reviewed in [4]). Previous metabolomics studies of pericytes have revealed their highly active energy metabolism, indicating the specific role of glucose and its uptake, ATP production from glucose catabolism and fatty acid oxidation [5] that can be potentially dysregulated upon a pathology [6].

We have recently demonstrated that pericytes covering GBM associated vessels (GA-Peris) can be distinguished from „normal“ pericytes covering vessels outside the tumor area by their expression profile, especially by the expression of epithelial to mesenchymal transition (EMT) factors like SLUG or TWIST [7]. We have further demonstrated that pericytes are prominently involved in the formation of GBM associated vascular proliferations and that GBM cells, by secretion of TGF-β, drive pericytes to change their growth morphology, induce proliferation and increase cell motility [8]. In consequence, we hypothesized that these functional alterations have an impact on the BBB integrity. Using an in vitro BBB model containing primary brain pericytes and microvascular endothelial cells as well as glioma cells or astrocytes, we demonstrate that the treatment of tight endothelial cell/pericyte layers with TGF-β, or co-culture of these layers with TGF-β secreting GBM cells, resulted in the disruption of this so far intact BBB.

Additionally, we employed ^{1}H-NMR spectroscopy-based metabolomics and RNAseq to determine the intracellular modulation of human brain microvascular pericytes (HBVP) to further underpin the biomolecular events taking place upon TGF-β treatment, and identified significant alterations of their metabolism. Energy, growth and several pathways were altered in HBVP upon TGF-β treatment compared to control, further indicating the fundamental changes in the pericyte´s environment.

2. Material and Methods

2.1. Cell culture

T98G glioma cells, the latter expressing high levels of TGF-β [9] were from the *American Type Culture Collection (ATCC, Manassas, USA).* SV-GA cells (a human astrocytic subclone of human fetal glial cells transduced with an origin-defective mutant of simian virus 40) were a kind gift of Walter Atwood (Brown University, Rhode Island, USA) and were described in [10]. SV-GA cells were tested for origin and integrity by staining against the astrocytic cells specific protein GFAP [11]. The cells were cultured, if not other noticed, in DMEM containing 10 % FCS, 1% penicillin and 100 µg/ml streptomycin (P/S; both Sigma Aldrich, Taufkirchen, Germany). Human brain vascular pericytes (HBVP) were purchased from ScienCell (Carlsbad, USA, # 1201-prf) and were cultured, if not other mentioned, on poly-L-lysine (PLL) coated plastic in pericyte medium (PM) in the presence of 2% FCS, 1% P/S and 1% pericyte growth supplements (PGS; containing apo-transferrin,

Preprints (www.preprints.org) | NOT PEER-REVIEWED | Posted: 20 December 2022 doi:10.20944/preprints202212.0342.v1

insulin, EGF, FGF, insulin growth factor (IGF)-1 and hydrocortisone; all from ProVitro, Berlin, Germany). HBVP were used up to passage 8.

To determine the doubling time of T98G and SV-GA cells, 1.000 cells were seeded in microtiter plates. After attachment, every 24 h hexadupletts of cells were stained with crystal violet as described [12]. Conditioned medium from T98G cells were prepared by seeding 200.000 cells. After attachment, the medium was changed to serum free MCDB-131 medium (EC-Medium; Sigma Aldrich) and was collected 24 h later.

2.2. Isolation of primary porcine brain microvascular endothelial cells

All animal experiments of this studies were covered by the approval of the Regional board Tübingen (notification to use animal organs for translational biomedical research, given to M. Schenk on December 22, 2017). Porcine brain microvascular endothelial cells (PBMVEC) were prepared from domestic pig brains of animals homing in the Tübingen animal facility. The brains were collected and transported on ice in PBS containing 153 mM NaCl, 5.6 mM KCl, 1.7 mM $CaCl_2$, 1.,2 mM $MgCl_2$, 15 mM HEPES, 0.01 g/ml BSA to the Laboratory. The cells were isolated using a slightly modified protocol previously described [13]. Meninges were removed, the cortex was cut into small pieces using scalpels, followed by homogenisation. The tissue was digested in collagenase II (Life Technology) for 60 min at 37°C, and purified by centrifugation in a 25% BSA solution, followed by a second enzyme treatment with collagenase/dispase (Roche) and DNase I for 50 min at 37°C. The cells were then seeded in 10 cm dishes in MCDB-131 supplemented with 50 µg/ml endothelial cell growth supplements (ECGS; K. Devraj, Edinger Institute, Frankfurt/Main, Germany; [14]), 1% P/S, 2mM L-glutamine, 0.01% heparin and 0.01% sodiumbicarbonate (all Sigma Aldrich) if not otherwise stated. After 4-14 h, puromycin (Sigma-Aldrich) was added to the media for the next 2 days to obtain a pure culture of PBMVECs. Dead cells were removed by washing and puromycin free EC medium was added for two further days. Afterwards the cells were collected and were stored at -80°C in FCS containing 10 % DMSO. The purity and origin of endothelial cells was determined by staining the cells for the microvascular endothelial cell specific protein ZO-1, the endothelial cell marker CD31 and claudin 5 (Figure 1B). Only first passage PBMVEC were used for experiments. During experiments the cells were cultivated in serum-depleted MCDB-131 supplemented with 1% PGS. All cells were cultured at 37°C and 5% CO_2 at 100% humidity.

2.3. The in vitro BBB model

To generate an intact and tight BBB *in vitro*, we used a modified protocol developed by Czupalla *et al*. [15]. PLL coated transwell inserts with a pore size of 0.33 µm were used (Thermo Fisher Scientific, Dreieich, Germany). 3.300 HBVPs were seeded in PM on the bottom side of the membrane and allowed to attach. Secondly, 35.000 PBMVEC were seeded on the top side of the membrane. The inserts were transferred into wells containing EC medium. At day 3 of culture, the medium was exchanged to freshly supplemented EC medium. The integrity of the barrier was assessed by transendothelial electric resistance (TEER) measurement using an EVOM-2 volt/ohm-meter and an adjusted STX2 electrode chopstick (World Precision Instruments, Germany) as previously described [16]. After a strong barrier developed (generally after 5 days of culture), the medium in the lower chamber was exchanged to serum deprived EC medium containing 1% of pericyte growth supplements (PGS), and recombinant human TGF-β1 and -β2 (PeproTech, Hamburg, Germany) was added at a final concentration of up to 12 ng/ml each. Alternatively, the inserts were transferred into new wells containing 200.000 T98G glioma or SV-GA astrocytic cells growing on the bottom. Before transferring the inserts, the medium of T98G or SV-GA cells were changed using serum-free EC-medium. TEER measurements were performed every day using a EVOM2 volt/ohm meter with adapted chopsticks (World Precision Instruments, Friedberg, Germany). The impedance and therefore the integrity of the barrier was calculated as described in [16] using the following equation: $TEER\ (\Omega * cm^2) = R\ (\Omega) * A\ (cm^2)$. To block TGF-β activity, a pan-TGF-β neutralizing antibody (clone

 doi:10.20944/preprints202212.0342.v1

1D11, # MA5-23795, ThermoFisher Scientific, Dreiech, Germany) was added to the TGF-β containing medium in a 100-fold excess.

To determine the effect of TGF-β on the BBB integrity in PBMVEC monocultures compared to PBMVEC/HBVP co-cultures, the cells were seeded as described above and 3 days later each 5 ng/ml TGF-β1 + -β2 was added. TEER measurement was then constantly measured in a period of 24 h on a CellZScope (NanoAnalytics, Münster, Germany) in accordance to the manufacturer´s protocol.

2.4. Immunocytochemistry and immunofluorescence

For immunocytochemistry, PBMVECs were seeded on fibronectin coated coverslips and allowed to attach. For staining for claudin 5 or ZO-1, the cells were fixed using 4% paraformaldehyde (PFA) and were permeabilized with 0. 1% Triton X-100/PBS as previously described [11]. For staining with CD31, the cells were fixed with 10% formaline and permeabilized with ice cold methanol according to the protocol supported by Novus (Novus Biologicals, Littleton, CO, USA). The following antibodies were used: anti-ZO-1 (# 61-7300, rabbit polyclonal, Invitrogen/Thermo Fisher Scientific, 1:200); Anti-Claudin 5 (Invitrogen, clone 4C3C2, mouse monoclonal, 1:100) and anti-CD31 (Biorad, #MCA1746GA, mouse monoclonal, 1:100) For the detection of ZO-1, as secondary antibody a DL488-coupled anti-rabbit IgG for claudin 5 and CD31 expression, a DL488-conjugated goat anti-mouse-IgG (all from Thermo Fisher) was used. Immunofluorescence was performed on a Zeiss LSM 710 confocal microscope, using the ZEN20 software (Zeiss, Oberkochen, Germany)

2.5. Freeze fracture electron microscopy

For electron microscopy, endothelial cells growing on the upper membrane side of *in vitro* BBB cultures were collected by mild trypsinization and scraping using a cell scraper. Cells from replicates were combined, then centrifuged, washed twice with PBS and the cell pellet was subsequently prepared for freeze fracture electron microscopy as described [17]. Alternatively, ECs were collected using a cell scraper, mounted between a sandwich of copper carriers, and plunge-frozen into a nitrogen-cooled liquid ethane/propane mixture using a Leica EM CPC (Leica Microsystems, Wetzlar, Germany). Afterwards, the sandwich carriers were transferred into a Leica EM BAF060 freeze-fracture and etching device. Samples were fractured at −162 °C and 1 × 10−7 mbar by chipping off the upper copper carrier, and subsequently deep etched for 5 min at −95 °C. Etched surfaces were shadowed with a 2 nm platinum-carbon coating applied at a 45° angle, stabilized by a layer of 20 nm carbon coating applied at 90°. The replicas were bound to a gold index grid using 0.5% Lexan polycarbonate plastic dissolved in dichloroethane (DCE). The DCE was allowed to evaporate at −20°C overnight, attaching the replica to the grid. The samples were thawed at room temperature and the carriers were removed. The replicas were cleaned by immersion in 70% sulfuric acid for 2 h, followed by 12% sodium hypochlorite (bleach) and double-distilled water for 1 h each. After drying, the Lexan film was removed by incubation in hot DCE. Analyses was performed using freeze fracture replicas observed in a Zeiss EM 10 (Zeiss, Oberkochen, Germany) or a FEI Tecnai G2 transmission electron microscope (FEI, Thermo-Fisher Scientific, Munich, Germany) at 120 kV, equipped with a digital 8-bit camera. Tight junctions (TJ) were labelled manually. TJ density (total length of TJs) and complexity (number of TJ branches) was analyzed using Image J (Fiji, NIH, Bethesda, USA [18]).

2.6. Metabolic analysis

The mitochondrial to glycolyctic ATP production was determined on a Seahorse™ XF96 Extracellular Flux Analyzer (Agilent Technology, Santa Clara, CA, USA) as previously described [19]. HBVP were seeded on poly-L-lysine coated Seahorse cell plates 24h prior to the experiment and were treated as indicated. During the experiment, the oxygen consumption rate (*OCR*) and extracellular acidification rate (ECAR) was measured before

Preprints (www.preprints.org) | NOT PEER-REVIEWED | Posted: 20 December 2022 doi:10.20944/preprints202212.0342.v1

any injection of mitochondrial toxins (refers to „basal state"). The wells were then injected sequentially with 8 µM oligomycin (Santa Cruz Biotechnology; refers to „minimal respiration"), 28 µM FCCP (Santa Cruz; refers to „maximal respiration"), and 40 µM antimycin A (Santa Cruz) plus 8 µM Rotenone (Sigma Aldrich; refers to „mitochondrial inhibition", and OCT/ECAR rates were measured again. Cell density was used for normalization. For this, after measurements the cells were washed with PBS, permeabilized with Triton-X-100 (5% w/v, Sigma-Aldrich) and stained with 4,6-diamidin-2-phenylindol (DAPI, Sigma-Aldrich). Cell density was determined by fluorescence intensity on a Tristar LB942 fluorescence reader (Berthold Technologies, Bad Wildbad, Germany). Data analysis was performed using the Seahorse Software Wave, the XF Real-Time ATP Rate Assay Reporter Generator (both Agilent Technologies), followed by further analyses using Excel.

2.7. ^{1}H-NMR spectroscopy-based metabolomics of HBVP intracellular metabolites

After TGF-β treatment, the cells were washed twice with ice-cold PBS, the adherent cells were shock-frozen with liquid nitrogen, placed on dry ice and further on wet ice. After addition of -80°C cold methanol the cells were scraped, collected, vigorously vortexed and stored at -80° C until extraction. The metabolite extraction and measurement techniques have been previously described [19]. Metabolites were annotated and quantified by ChenomX NMR Suite 8.5 software containing the additional human metabolome data base (HMDB) 600 MHz library. All data was normalized by a reference sample with probabilistic quotient normalization (PQN) to account for dilution effects.

2.8. RNA sequencing

For RNASeq, HBVP were treated as indicated. Total RNA was prepared using the Nucleo Spin RNA Mini isolation kit with DNA removal column (Machery-Nagel, Düren, Germany). RNASeq was performed at the c.ATG facility of the NGS Competence Center Tübingen (NCCT) using the QuantSeq 3' mRNA-Seq Library Prep FWD and the NovaSeq 6000 SP Reagent Kit v1.5 with 200 cycles and 15 million cluster (both kits from Illumina, Berlin, Germany). Primary analyses were performed by sequencing data demultiplexing, secondary analyses by RNA gene expression per sample using the e!Ensembl reference genome, followed by differential gene expression for the sample groups.

2.9. Combined metabolomics and RNA-seq pathway analysis

Metabolite and gene, joint-pathway analysis was performed based on Kyoto encyclopedia of genes and genomes (KEGG) pathway database of integrated metabolic pathways that have both metabolites and metabolic genes. A combined query integration method using metabolite and gene fold change values from TGF-β-treated samples compared to control was performed via the MetaboAnalyst online platform [20]. Hypergeometric test was selected for enrichment analysis. Degree centrality was used as the topology measure.

2.10. Statistics

All BBB experiments were performed independently at least thrice with up to 10 technical replicates per experiment unless mentioned otherwise. Statistics were done using GraphPad Prism 9.4.1. or Excel. For TEER analyses data from untreated cells served as control, all replicates from each treatment group were combined for analyses. The t-test for unpaired samples, or the analysis of variance (ANOVA) test, followed by the Bonferroni post-hoc test for multiple testing, was used. Results are represented as mean ± standard error mean (SEM). *P*-values of <0.05 are considered as statistically significant (ns: not significant; * $P < 0.05$, ** $P < 0.01$, *** $P < 0.001$, **** $P < 0.0001$). For metabolomics analysis, the MetaboAnalyst 5.0 web server (R-based online analysis tool, www.metaboanalyst.ca [20]) using unpaired t-test analysis with false discovery rate (FDR)-corrected p value threshold of 0.05, and fold change (FC) threshold of 1.2. Then the student's t-test was applied to compare metabolite concentrations between the control and TGF-β treated cells

Preprints (www.preprints.org) | NOT PEER-REVIEWED | Posted: 20 December 2022 doi:10.20944/preprints202212.0342.v1

using GraphPad Prism 9.3.1. software. We used principal component analysis (PCA), pattern hunter, heatmap, and joint-pathway analysis tools for data visualization. Heat map shows auto scaled concentration values (-2;2) with clustered features by Ward clustering algorithm based on Euclidean distance measure. Pattern hunter correlations are based on Pearson r distance measure. Joint-pathway analysis is based on 84 metabolite sets based on KEGG human metabolic pathways (Oct. 2019).

3. Results

3.1. Co-cultures of primary endothelial cells and pericytes develop a tight BBB

In our experiments, we used an *in vitro* BBB model that combines the culture of primary PBMVEC and HBVP and allows co-culture with other cells, the addition of conditioned medium or the addition of cytokines like TGF-β (Figure 1A). First, we validated the origin and purity of isolated PBMVEC by staining with CD31, claudin 5 and ZO-1. As shown in Figure 1B, PBMVEC were positive for all three proteins whilst LN-308 GBM control cells were negative. Isolated PBMVEC had a purity of higher than 95%. PBMVEC alone developed a more leaky barrier, whereas after 5 days co-cultured PBMVEC and HBVP created a tight barrier (Figure 1C, Supplementary Figure 1). To show that our model is feasible to measure exogenous effects influencing the barrier integrity, and as it is described that *in vivo* brain astrocytes positively, and glioma cells negatively influence the integrity of the BBB, we tested whether this can be reproduced in our model. For this we transferred barrier-tight PBMVEC/HBVP co-culture membranes into cell culture wells containing immortalized astrocytic SV-GA or T98G GBM cells growing on the bottom of the well. These cell lines have been chosen to avoid artefacts induced by differences in cell proliferation of astrocytic and glioma cells since both SV-GA and T98G cells showed nearly equal doubling times (approximately 56 +/4 h for SV-GA and 59 +/- 6.6 h for T98G cells). As shown in Figure 1D, the co-culture of barrier-intact PBMVEC/HBVP layers with SV-GA cells further enhanced, whereas the co-culture with T98G cells significantly reduced the integrity of the barrier, indicating that the *in vitro* BBB model is feasible to determine influences on BBB integrity and leakiness.

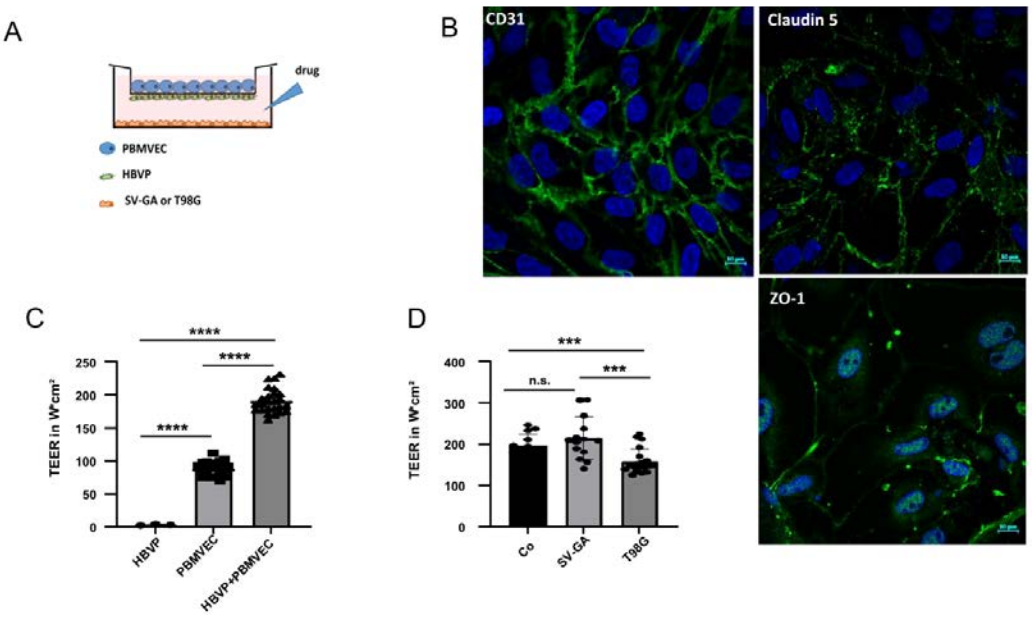

Figure 1: The *in vitro* blood-brain-barrier (BBB) model. (A) Scheme of porcine brain microvascular endothelial cells (PBMVEC), human brain microvascular pericytes (HBVP) and SV40 large T-antigene immortalized astrocytic cells (SV-GA) or T98G glioblastoma cell line localization in the BBB co-culture model co-culture. (B) CD31, Claudin 5 and ZO-1 staining of isolated PBMVEC (bars = 10 µm). (C) The cells were cultivated as described in the material and methods part either as monocul-

 doi:10.20944/preprints202212.0342.v1

tures (HBVP on the bottom insert membrane; PBMVEC on the top insert membrane) or as co-cultures. After 5 days, the membrane integrity was determined by TEER measurement (n=3, each up to 10 replicates, SEM, t-test, **** $p<0.0001$). (D) Co-culture of barrier-tight BBB-layers (containing PBMVEC and HBVP) with SV-GA or T98G cells. TEER was performed 24 h after co-culture (Co.: no additional cells were seeded; n>7, SEM, t-test, *** $p<0.005$). Co-culture with astrocytic cells strengthen, with glioma cells weakens barrier integrity.

3.2. TGF-β treatment of HBVP negativels modelates the integrity of the BBB

We have recently published that TGF-β modulates the function of HBVP. It induces cell motility, proliferation and additionally modulates the pericytic growth pattern and morphology [8]. In this regard, we were interested whether these changes are associated with the breakdown of the BBB. For this, we added TGF-β into the bottom chamber of wells containing barrier-intact PBMVEC/HBVP layers, or transferred these cultures into new cell culture wells containing T98G cells growing on the bottom. T98G cells were chosen since these cells secret high amounts of both TGF-β1 and -β2 [9]. The specificity of TGF-β as a modulator of the BBB integrity was determined by the addition of the TGF-β neutralizing antibody 1D11. Addition of TGF-β1 plus -β2 at a concentration of >5 ng/ml each resulted in a significant decrease of the barrier density (Figure 2A, B). A trend towards a reduced barrier density was also observed if barrier-tight PBMVEC/HBVP membranes were transferred into wells containing T98G GBM cells (Figure 2C). The barrier leakiness induced by TGF-β or co-culturing the membranes with T98G GBM cells could be, at least partially, reverted by the addition of 1D11 (Figure 2B, C). We next examined whether the protective and supporting function of HBVP on barrier integrity was influenced by TGF-β. For this we compared the effect of TGF-β on PBMVEC monocultures with that on PBMVEC/HBVP co-cultures but already added TGF-β 48h after seeding, a time point a dense BBB was not completely built up. As shown in Figure 2 D-E, addition of TGF-β inhibited barrier tightening both in mono- and co-cultures. In addition, the supporting function of pericytes in the development of barrier tightness was reduced to some extent by TGF-β as shown by the additional TEER reduction in co-cultures (Figure 2E).

Preprints (www.preprints.org) | NOT PEER-REVIEWED | Posted: 20 December 2022 doi:10.20944/preprints202212.0342.v1

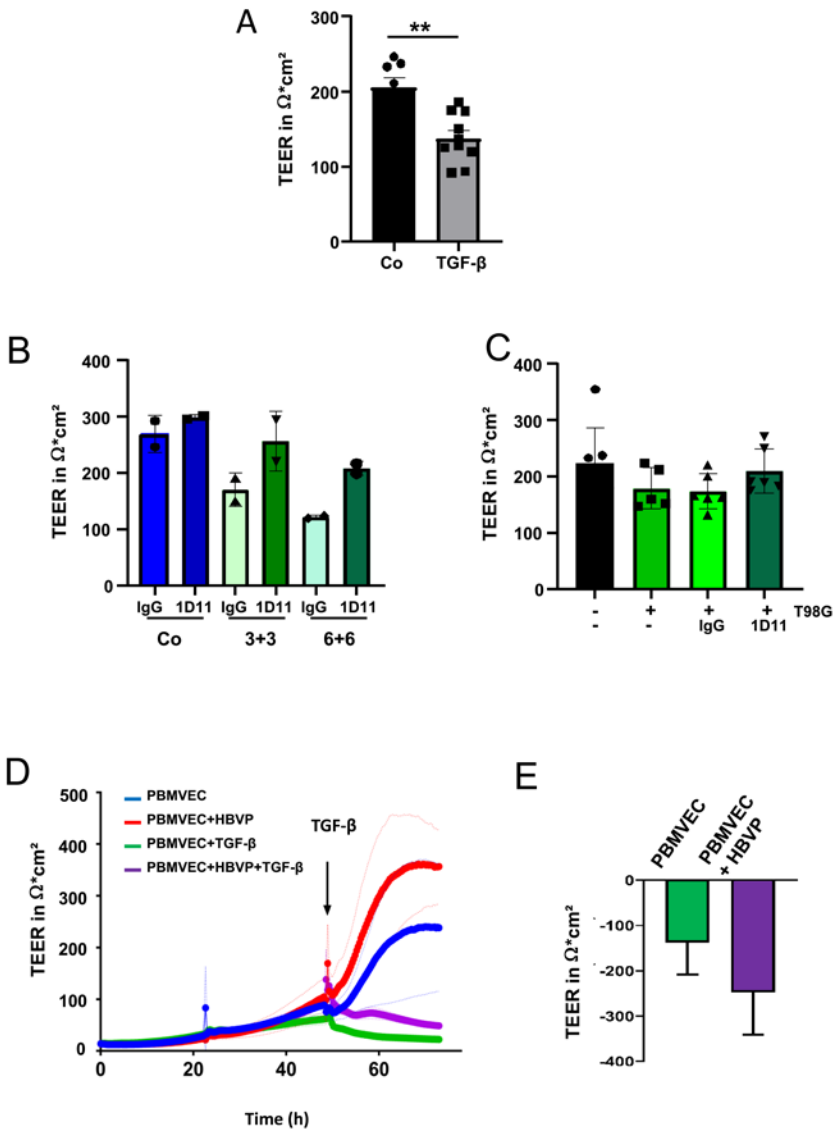

Figure 2: TGF-β negatively modulates the integrity of the BBB *in vitro*. (A) TGF-β negatively modulates the integrity of the barrier. Addition of TGF-β1 plus -β2 (each 5 ng/ml) into the bottom chamber (HBVP cell membrane side) of barrier-tight BBB layers. 24 h later the integrity of the barrier was determined by TEER (Co: sham treatment; n=4, each 2 technical replicates, SEM, t-test, ** $p < 0.01$). (B) The cells were treated with TGF-β1 plus -β2 (each 3 or 6 ng/ml) in the absence or presence of the pan-TGF-β neutralizing antibody 1D11 (1 µg/ml). Addition of 1D11 reverted the TGF-β mediated reduction of the BBB integrity (Co: sham treatment, n=2, each one replicate, SD). (C) Intact barrier dense BBB layers were transferred into new wells containing either no cells (black bar) or T98G cells (green bars) as well as no antibody (-), 1D11 antibody or an isotype control (IgG, each 1 µg/ml). 24 h later TEER measurement was performed (n=3, each 2 replicates, SEM, t-test). (D) PBMVEC monoculture and PMBVEC/HBVP co-culture membranes were treated with TGF-β1 plus -β2 (each 5 ng/ml) 48 h after seeding. TEER measurement was performed as described in the methods part (one out of three independent experiments is shown, light colored lines indicate the SD of technical replicates). (E) Differences in the reduction of TEER in PBMVEC mono- and PBMVEC/HBVP co-cultures after addition of TGF-β1 plus -β2 (each 5 ng/ml; n=3, SD, p= 0.18)

To structurally demonstrate the effect of TGF-β on the BBB breakdown, we isolated PBMVECs growing on the upper HBVP/PBMVEC co-culture-membrane 24 h after TGF-β treatment and determined the amount of tight junctions (TJ), typical structures of endothelial cells at an intact BBB, by freeze fracture electron microscopy. The amount of TJ density and complexity in PBMVEC was notably reduced 24 h after the addition of TGF-β (Figure 3).

Preprints (www.preprints.org) | NOT PEER-REVIEWED | Posted: 20 December 2022 doi:10.20944/preprints202212.0342.v1

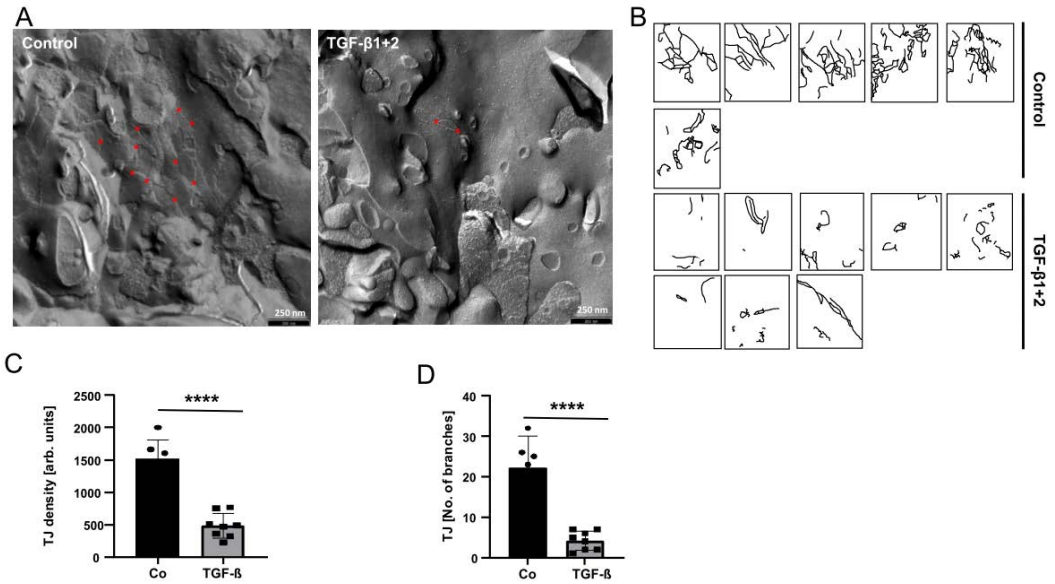

Figure 3: TGF-β treatment of HBVP reduced the amount and complexity of TJ in endothelial cells. (A) TGF-β1 plus -β2 (each 10 ng/ml) were added into the bottom chamber of wells containing intact BBB layers. 24 h later, PBMVEC growing on the upper part of the membrane were collected and prepared for freeze fraction electron microscopy. Red stars exemplarily indicate TJ branches. (B) TJs were manually labelled in different visual fields. Exemplary, one photograph is shown (n=2, in total 4 replicates). (C/D) Quantification of TJs density (C) and complexity (D) (n=6 visual fields for controls, n= 8 for TGF-β).

3.3. TGF-β treatment leads to a distinct metabolite profile, pathway alterations, and gene expression patterns in HBVP

Recent studies have revealed the relevance of metabolic pathways in endothelial and mural cells, this controlling vascularization. The contribution of specific metabolic programs to the regulation of cell-state decisions has been investigated extensively in endothelial cells (for review see [21]). However, metabolic changes in pericytes, and especially in GBM associated pericytes have undergone very limited analysis to date. We primarily observed changes in the metabolic activity of pericytes that were treated with TGF-β, this associated with an elevated proliferation and motility, with morphological alteration of these cells [8] as well as with the breakdown of an intact barrier (Figure 2). As it has been described that the activation of peripheral pericytes was associated to changes in energy generation, especially the switch of ATP production by oxidative phosphorylation towards glycolysis [22], we first determined mitochondrial and glycolyic ATP production upon TGF-β treatment. Indeed, a trend towards glycolytic ATP production was observed (Figure 4 A). Further ^{1}H-NMR spectroscopy-based metabolomics analysis quantified a total of 42 metabolites whose concentration was altered by TGF-β in HBVPs (Figure 4B, C, Supplementary Figure 2). From those, 9 metabolites namely aspartate, glycine, O-phosphocholine, glutamate, UDP-glucose, citrate, glucose, acetate and inosine concentration changes were identified as statistically significant by univariate statistical analysis with $p < 0.05$ (FDR approved) and fold change threshold > 1.2, when comparing TGF-β treated cells to control (Figure 4 B, C and Supplementary Figure 2 D). Furthermore, 6 metabolites namely pyroglutamate, tyrosine, lysine, alanine, leucine (the branched-chain amino acids), and NAD^{+} had altered concentrations based on unpaired t-test (Supplementary Figure 1 D, E).

Preprints (www.preprints.org) | NOT PEER-REVIEWED | Posted: 20 December 2022 doi:10.20944/preprints202212.0342.v1

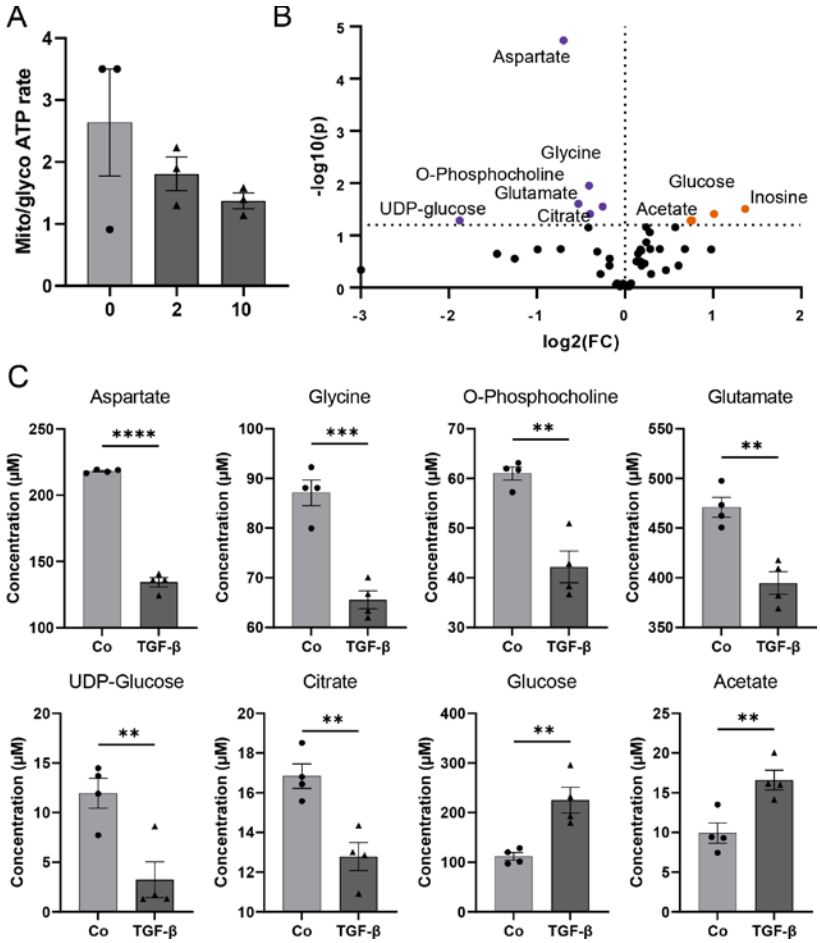

Figure 4: Metabolomics analysis of HBVP upon TGF-β treatment. (A) Determination of mitochondrial to glycolytic ATP production at different TGF-β concentrations using respiratory analysis. HBVP were treated with TGF-β (2 or 10 ng/ml) for 16 h or were left untreated (n=3, each 6 technical replicates, SEM). (B) Volcano plot visualizing most significant metabolite concentration increase (orange dots) and decrease (purple dots) upon TGF-β treatment compared to control for $p<0.05$, false discovery rate (FDR)-corrected data with fold change (FC) threshold >1.2 (n = 4). (C) Bar plots with individual replicate points and SEM of the most significant metabolite changes upon TGF-β treatment (black triangles) (n = 4): aspartate, glycine, O-phosphocholine, glutamate, UDP-glucose and citrate concentrations were decreased compared to control (black dots), while glucose and acetate concentrations increased upon TGF-β treatment, based on parametric, unpaired t-test, ** $p < 0.01$, *** $p < 0.001$, **** $p < 0.0001$.

We further investigated correlation patterns (Spearman's R) between the metabolites in our quantified dataset. Pattern hunter analysis of the glycolysis metabolite glucose revealed that inosine, leucine, isoleucine, valine (branched-chain amino acids), lysine, acetate, pyroglutamate, phenylalanine, tyrosine, glutamine concentrations follow the same pattern in the dataset as glucose. Meanwhile, aspartate, glycine, citrate, NAD^+, UDP-glucose, O-phosphocholine, glutamate and ATP negatively correlated with glucose (Figure 5 A). Furthermore, when correlated with the TCA cylcle metabolite citrate, O-phosphocholine, glycine, UDP-glucose, aspartate, UDP-galactose, UDP-glucuronate, oxidized glutathione (GSSG), NAD+, and 1-methylnicotinamide were positively correlated to citrate concentration (Figure 5 B). Inosine, acetate, glucose, pyroglutamate, alanine, formate, lactate, sucrose, lysine, tyrosine, leucine, N-methyl-D-aspartate, glutathione, and isoleucine negatively correlated to citrate concentration patterns in the dataset (Figure 5 B).

Preprints (www.preprints.org) | NOT PEER-REVIEWED | Posted: 20 December 2022 doi:10.20944/preprints202212.0342.v1

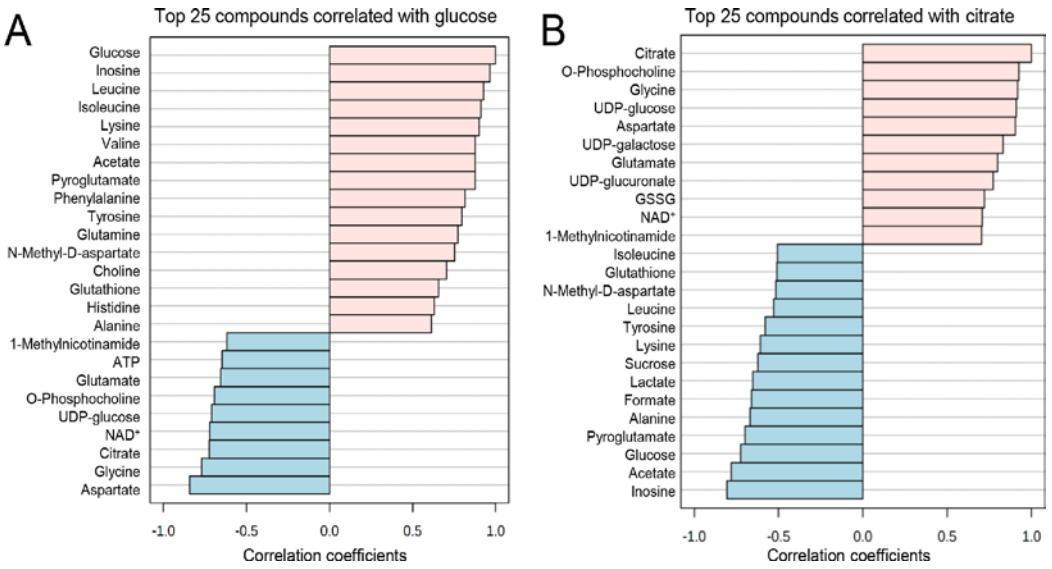

Figure 5: Pattern hunter analysis of glucose and citrate. (A) Glucose concentration pattern changes positively correlate with inosine, leucine, isoleucine, lysine, valine, acetate, pyroglutamate, phenylalanine, tyrosine, glutamine, N-methyl-D-aspartate, choline, glutathione, histidine, and alanine, while negatively correlate with aspartate, glycine, citrate, nicotinamide adenine dinucleotide $(NAD)^+$, uridine diphosphate (UDP)-glucose, O-phosphocholine, glutamate, adenosine triphosphate (ATP) and 1-methylnicotinamide. (B) Citrate positively correlates with O-phosphocholine, glycine, UDP-glucose, aspartate, UDP-galactose, UDP-glucuronate, oxidized glutathione (GSSG), NAD^+, and 1-methylnicotinamide; and negatively correlates with inosine, acetate, glucose, pyroglutamate, alanine, formate, lactate, sucrose, lysine, tyrosine, leucine, N-methyl-D-aspartate, glutathione, and isoleucine concentration patterns, based on Pearson r distance measure (n = 4, two-group comparison).

In line with metabolomics analysis, RNA sequencing identified alterations in the expression pattern of genes that are involved in the regulation of energy generation and metabolic pathways, such as proline rich 5 (PRR5L, 4.9 fold upregulated by TGF-β), solute carrier family 46, member 3 (SLC46A3, 4.9 fold upregulated by TGF-β), peroxisome proliferator-activated receptor gamma, coactivator 1 alpha (PPARGC1AC, 3.2 x down), NADPH oxidase 4 (NOX4, 5.9 x up). Additionally, several genes important for the maintenance of the BBB like the transcription factor 1 forkhead box S1 (FOXS1, 8.2 x up), the G protein-coupled receptor 183 (GPR183, 7.1 x up) and sparc/osteonectin, cwcv and kazal-like domains proteoglycan 1 / testican (SPOCK1, 2.x up), or that are indicators for disfunctional blood vessels or an impaired BBB (e.g. ADAM metallopeptidase with thrombospondin type 1 motif, 6, ADAMTS6, 2.6 x up; endothelial cell-specific molecule 1 / endocan, ESM1, 7.6 x up) have been identified to be differentially regulated by TGF-β. In addition to metabolic genes and genes that are involved in BBB integrity, several genes are differentially expressed that are involved in processes of the EMT and EMT associated processes like cell migration, invasion and proliferation (Supplementary Table 1 and 2).

3.4. Joint-pathway analysis illustrates further pathways dysregulated upon TGF-β treatment

Finally, we performed a joint-pathway analysis combining metabolite and gene expression data, using fold change values of 42 metabolites and genes that were obtained from TGF-β treatment samples and compared to control. By using MetaboAnalyst 5.0 online tool for joint-pathway analysis [20], and selecting human organism (homo sapiens), we identified 9 significantly changed pathways: glycerolipid metabolism, valine, leucine and isoleucine biosynthesis (branched chain amino acid (BCAA) biosynthesis), glycerolphospholipid metabolism, amino sugar and nucleotide sugar metabolism, aminoacyl-tRNA biosynthesis, ascorbate and aldarate metabolism, glycolysis or gluconeogenesis,

Preprints (www.preprints.org) | NOT PEER-REVIEWED | Posted: 20 December 2022 doi:10.20944/preprints202212.0342.v1

histidine metabolism, and alanine, aspartate and glutamate metabolism (Figure 6, Supplementary Table 3). Joint-pathway analysis of differentially regulated genes and metabolites indicated a close network of pathways involved in processes of cell growth which could be connected to angiogenesis, vessel structure, EMT and proliferation as well as energy and redox metabolism.

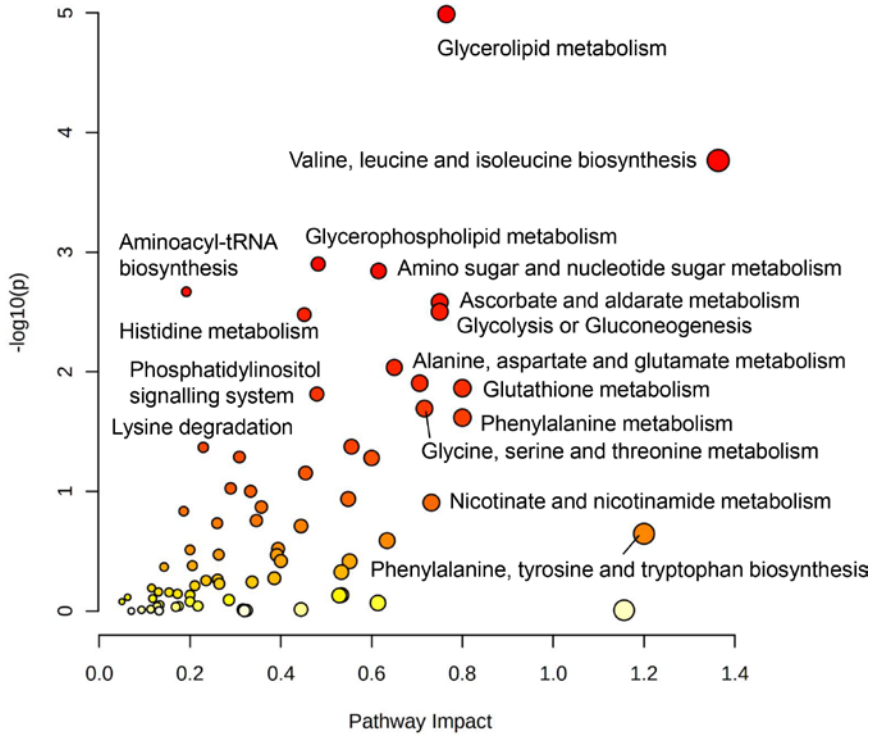

Figure 6: Joint pathway analysis of ^{1}H-NMR spectroscopy-based metabolomics and RNAseq gene fold change data. Pathway analysis indicates the most significantly changed metabolic pathways. Glycerolipid metabolism, branched-chain amino acid (BCAA) metabolism of valine, leucine and isoleucine biosynthesis, glycerophospholipid metabolism, amino sugar and nucleotide sugar metabolism, ascorbate metabolism, glycolysis or gluconeogenesis, and alanine, aspartate and glutamate metabolism, were most affected based on Kyoto encyclopedia of genes and genomes (KEGG) pathway database. For joint-pathway analysis data from metabolomics (n=4) and RNAseq (n=4) were used.

4. Discussion

The regulation of the BBB integrity by pericytes in GBM is currently of great interest as pericytes are functionally modulated and activated by glioma cells [8, 23, 24]. Well-established protocols for the isolation of brain microvascular pericytes and endothelial cells open the possibility to study the pericyte influence on the BBB integrity *in vitro* [25, 26]. TEER measurement revealed a barrier integrity increasing effect, finally resulting in a tight barrier, when PBMVEC, described to be feasible cells to study BBB integrity in vitro [27], separated by a 0.33 μm pore membrane, were co-cultured with HBVP. Only a small, barrier increasing effect was achieved if astrocytes were presented, yet a significant decrease, if TGF-β secreting GBM cells were presented to the membranes during the development of the barrier (Figure 1D). One limitation of our model might be the cross-species usage of porcine endothelial cells and human pericytes. In this respect, none of momentarily available human in vitro BBB models meet all the criteria of in vivo BBB models. Furthermore, cross-species BBB models have been successfully used in the past [28]. We believe that our data show the feasibility of the in vitro BBB model to determine whether GBM secreted factors will influence the BBB integrity.

 doi:10.20944/preprints202212.0342.v1

We have previously shown that glioma vessel-associated pericytes (GA-Peris) expressed key EMT factors like SLUG and TWIST [7]. Additionally, TGF-β, a classical inductor of EMT processes, which is highly secreted by glioma cells, induced SLUG expression in HBVPs, in parallel with the induction of proliferation, cell motility and alpha smooth muscle cell actin (αSMA) expression, resulting in the activation of pericytes [7, 8, 29]. This opened the discussion whether these TGF-β-mediated functional changes and activation of pericytes influences the BBB integrity. Thanabalasundaram et al. have shown that pericytes differentiated in the presence of TGF-β and subsequently co-cultured with endothelial cells were not able to establish a tight BBB [30]. In our present study we demonstrate that not only the establishment of an intact BBB was disturbed by TGF-β, but also the integrity of a so far intact barrier was destroyed, putatively by a TGF-β-mediated prohibition of the supporting function of pericytes in the maintenance of the BBB. Similar results were observed when T98G GBM cells were co-cultured adjacent to the pericytes. Our observations are in line with the observation of Atis et al. who recently published that inhibition of the TGF-β receptor type I prevented BBB disruption in hypertensive mice [31]. We observed reduced BBB integrity when we culturing "BBB-intact" inserts in the presence of T98G. The effects were less notable as when adding recombinant TGF-β into the pericytic compartment. However, this might be explained by the fact that we exchanged the medium in the compartment containing T98G cells to serum-deprived EC-medium just before transferring the BBB-dense inserts (Figure 1A). Therefore, no TGF-β was present at the begin of the treatment. Whilst the TGF-β concentration produced by T98G cells increased during co-culture, it might be even low at the time point of measuring the barrier integrity 24 h later and might be also lower than the concentration of recombinant TGF-β1 plus -β2 we used when initially adding this cytokine to the lower compartment. The observed effects on BBB integrity were TGF-β-dependent since neutralization of TGF-β activity at least partially abolished this effect (Figure 2B, C). Since we only performed short-term TGF-β treatment of pericytes which is not sufficient to alter the differentiation state of these cells [30], our data suggest that there is a direct effect of TGF-β in endorsing pericyte barrier functions of endothelial cells in addition to its role in differentiation. This is strengthened by our observation that a TGF-β-mediated complete breakdown of the barrier was observed in both PBMVEC mono- as well as in PBMVEC/HBVP co-cultures, indicating that the supporting function of pericytes was also inhibited by TGF-β (Figure 2 D, E). This is further supported by the observation that the amount and complexity of TJs was significantly reduced in co-cultured endothelial cells (Figure 3). However, we cannot completely exclude direct effects of TGF-β on endothelial cells using barrier tight PBMVEC/HBVP membranes for our analyses. Even if adding TGF-β to the pericytic compartment or co-culturing barrier-tight HBVP/PBMVEC membranes with glioma cells at the time point we measured an intact and tight barrier function (Figure 1 C,D, Figures 2 A-C, Supplementary Figure 1), there might be some additional TGF-β effects on PBMVECs.

It is well known that TGF-β is able to increase glycolysis in GBM cells (for a review refer to [32]). Here, we identified significant changes in the concentrations of a variety of metabolites as well as in the expression of metabolic pathways associated with this phenomenon in TGF-β treated HBVP. Based on the trend from mitochondrially towards glycolytically generated ATP in HBVPs upon TGF-β treatment (Figure 4A, C, Supplementary Figure 2) we interpreted the changes of metabolites that were found to be significant with an FDR adjusted p-value < 0.05. We hereby want to highlight the intracellular increase of glucose and decrease of citrate under TGF-β treatment as key findings as this supports a switch in energy production from mitochondrial oxidative phosphorylation (OxPhos) towards glycolysis. A similar observation has been previously described for activated peripheral non brain pericytes, associated with the barrier integrity ([22] and reviewed in [5]). The postulated TGF-β-mediated switch from OxPhos to glycolysis we observed in HBVPs was further associated with altered concentrations of key metabolites from the pentose phosphate pathway (PPP) which is in line with the observed metabolic shift. The shift towards PPP subsequently feeds nucleotide synthesis necessary for proliferation and

 doi:10.20944/preprints202212.0342.v1

NADPH to maintain redox and counteract oxidative stress (Figures 4, 5 and Supplementary Figure 2). Furthermore, glycerolipid and glycerophospholipid metabolism (also known as Kennedy pathway-related metabolites) and gene expression changes suggest enhanced cell membrane synthesis as well as amino-tRNA and BCAA biosynthesis pathway changes point towards altered protein synthesis (Figures 5, 6). This fits well to our former observations that pericytes are the most prominent cells in GBM associated vascular proliferates, and that HBVPs that underwent a TGF-β mediated EMT reprogramming showed elevated proliferation [7, 8]. Alterations in phospholipid metabolism and Kennedy pathway have been also previously reported as a marker for recurrent glioblastoma [33]. In addition, enzymes modulating the energy metabolism of cells are differentially regulated: SLC46A3 (4.9 x upregulated by TGF-β) has been suggested to be involved in the plasma membrane electron transport (PMET), a plasma membrane analogue to the mitochondrial electron transport chain that contributes to energy production by supporting glycolytic ATP production [34]. PRR5L modulates mTORC2 activity which is known to regulate glucose uptake, glycolysis and the PPP [35]. Nicotinamide adenine dinucleotide phosphate oxidase (NOX)-4, 5.9 x upregulated by TGF-β, is highly upregulated in stroke-associated pericytes, and its overexpression in pericytes induces a breakdown of the BBB by upregulating matrix metalloproteinase (MMP)-9 [36], the latter also associated with capillary damage during ischemia [37]. In contrast, PPARGC1 mRNA, coding for PGC-1α, was 3.2-fold downregulated by TGF-β. PGC-1α is transcriptional key regulator of energy metabolism and a master regulator for mitochondrial biogenesis [38]. This supports our observation that ATP production was shifted towards glycolysis by TGF-β in HBVPs. Besides, PGC-1α participates in the regulation of carbohydrate and lipid metabolism which in TGF-β treated HBVPs we also found to be modulated [39]. However, not only the energy metabolism of HBVPs was modulated by TGF-β. In fact, increased concentrations of BCAA have been seen as important drivers of cell migration and mTORC1 activation [40] with mTORC1 hyperactivation has been linked to promotion of angiogenesis in endothelial cells [41], and an elevated migration of HBVPs was observed in GA-Peris that underwent an EMT-like transition [8]. Pericytes are particularly sensitive to oxidative stress [42-44], it would therefore be interesting to investigate the impact of a shift from OxPhos to glycolysis on the oxidative state in these cells. A first hint that metabolic changes in TGF-β treated HBVP are connected to oxidative stress are highlighted by changes to the glutathione and GSSG levels (Supplementary Figure 2A).

Joint metabolomics and RNAseq pathway analysis identified a network of pathways that are important for angiogenesis, vessel structure, cell motility, anabolic and catabolic processes as well as EMT signaling that were modulated in GA-Peris [7, 8]. To better understand these processes in detail, further studies disturbing or blocking different metabolic, motility or proliferation-associated pathways are necessary to unravel the detailed connections of changes in metabolite concentrations to (i) BBB integrity, (ii) vessel structure, (iii) pericyte activation or (iv) motility, and to feaze which of the alterations in GA-Peris is connected to modulations of (v) the vessel structure or (vi) to the BBB maintenance, or (vii) if it is the GBM-induced homeostasis breakdown in GA-Peris that is responsible for the tumor-associated chaotic vessel structure and BBB breakdown. This might be done by the intervention of different metabolic, motility or proliferation associated pathways. Additionally, the portion of TGF-β-induced changes in pericytes in regard to their supporting function in BBB maintenance has to be evaluated as it is known that TGF-β also has direct effects on endothelial cells [45]. This might be done by the deletion of TGF-β receptors in endothelial cells or by the disruption of the intracellular TGF-β signaling in these cells. Nevertheless, we believe that TGF-β further modulates BBB supporting functions of pericytes as the effect of TGF-β on pericytes is similar to that on endothelial cells. In both cell types TGF-β induces a “epi/endothelial” to mesenchymal transition signature [7, 8, 46]. However, another study points toward a protective role of TGF-β on brain endothelial cells, whereas a third report stated opposite effects [47, 48]. In the latter study, immortalized brain capillary endothelial cells were used. However, in our hands these immortalized cells, in contrast to first passage primary PBMVEC, failed to generate a tight,

 doi:10.20944/preprints202212.0342.v1

intact barrier when co-cultured with HBVP and therefore might not be an optimal model to measure even small effects how integrity of the BBB can be influenced by GBMs.

This study provides novel insights into how metabolic changes in brain pericytes are associated with their function and might thus be used to develop new strategies targeting angiogenic processes to treat GBM. In this regard one might think to normalize tumor vascularization, as this has been shown to improve glioblastoma outcome [49] and might lead to a functional vessel structure, function and an intact BBB. This, in succession, diminishes brain edema, an important neurological issue of GBM that makes the usage of corticosteroids indispensable, but on the other hand interfere with recently developed immunotherapeutic approaches. Furthermore, an intact tumor vessel structure upon vessel normalization might improve the transport of BBB passable drugs into the tumor tissue [50]. Future in vitro and in vivo studies including the perturbation of the metabolic pathways we identified in this study are needed to unravel the complex mechanism of violated GBM angiogenesis and to develop strategies for vessel normalization.

5. Conclusion

In summary, our data indicate that glioma-secreted TGF-β not only results in dysfunctional and leaky new-built vessels during tumor-associated neoangiogenic processes, but also leads to the disturbance of an intact BBB by modulating the supportive function of pericytes. Metabolic alterations in the pericytes are associated with the breakdown of the BBB, shifting the cells energy generation from OxPhos towards glycolysis, and leading to modification in several metabolic associated pathways. This putatively influences several functional processes in these cells that finally modulate their functional behavior. Further animal models will show whether the inhibition of TGF-β has an impact on the BBB integrity in the tumor area also *in vivo*.

Supplementary Materials: Supplemental data for this article is available as 2 supplementary figures and 3 supplementary tables.

Supplementary Figure 1: PBMVEC and HBCPs were seeded on membranes as described in the Material and Methods part. The tightness of the barrier that was generated was determined by measuring TEER. A stable and dense barrier was generated 5 days after coculture (n=3, two to six replicates each, SD).

Supplementary Figure 2: Metabolomics analysis of HBVP upon TGF-β treatment. (A) Heatmap of all quantified metabolites in VBHP, illustrated as auto scaled concentration values (-2;2), features clustered by Ward clustering algorithm based on Euclidean distance measure. (B) Principal component analysis (PCA) scores plot illustrating the treatment and sample group separation based on different metabolic profile, PC 1 61.8%, PC 2 25.4%. (C) PCA bi-plot indicates specific metabolites that drive the group separation: aspartate and glutamate are more associated to control group, while glutamine, pyroglutamate, glucose, lactate and formate are more associated with the TGF-β treatment group. (D) Bar plots with visualizing individual replicate points and SEM of significant metabolite changes upon TGF-β treatment (black triangles), in addition to Figure 4 C: inosine, pyroglutamate, tyrosine, lysine, alanine and leucine concentrations were increased compared to control (black dots), while NAD^+ concentration was reduced in TGF-β treatment group based on parametric, unpaired t-test, * $p < 0.05$, ** $p < 0.01$. (E) Volcano plot visualizing most significant metabolite increased concentrations (orange dots) and decreased concentrations (purple dots) upon TGF-β treatment compared to control for $p<0.05$, with fold change (FC) threshold 0.8.

Supplementary Table 1: Upregulated genes with a log fold change of > 2 in TGF-β treated HBVP.

Supplementary Table 2: Downregulated genes with a log fold change of >2 in TGF-β treated HBVP.

Supplementary Table 3: **Joint-pathway analysis of metabolomics and RNA sequencing datasets.** Most significantly changed pathways of TGF-β vs. control, based on joint-pathway analysis by metabolite concentrations and gene expression fold change, top 14 metabolic pathways.

 doi:10.20944/preprints202212.0342.v1

Acknowledgments: We thank Hartwig Wolburg (Prof. emeritus, Institute for Pathology and Neuropathology, University Hospital Tübingen) for his help for the quantification of TJs, and Ria Knittel for technical help with the freeze fracture. We also thank Dr. Martin Schenk (Experimental Surgery, University Hospital Tübingen) for the provision of pig brains. We thank Werner Siemens Foundation, Prof. Dr. Bernd Pichler for financial support, and Miriam Owczorz for excellent technical support. MM would like to thank the Luxembourg National Research Fond (FNR) for the support (FNR PEARL P16/BM/11192868 grant).

Institutional Review Board Statement: All research meets ethical guidelines and adheres to the legal requirements of the study country. In this study, no patient material was used, therefore no ethics approval and patients consent is needed. We do not perform animal experiments in this study. However, the usage of animal material (in this study organ [brain] removal from domestic pigs and preparation of porcine brain pericytes) was covered by the Regional board Tübingen ("Anzeige": Notification to use animal organs for translational biomedical research, given to M. Schenk on December 22, 2017).

Funding: The study was funded by a scholarship to LS from the IZKF Promotionskolleg of the Medical Faculty, University of Tübingen.

Availability of data and materials: The datasets generated during and/or analyzed during the current study are available on the Mendeley data repository (*the accession number will be added as soon as the paper has been accepted*).

Authors' contribution: UN designed and supervised the study. MM, CT, and UN wrote the manuscript. LS, RS, LZ, JE, FKB, AB, AG, CM, PFB, and CT performed experiments and analyzed data. JCF and KD provided material and technical training., MM, CT and UN discussed data. All authors read the manuscript.

Conflicts of interest: The authors declare that they have no competing interests.

Abbreviations:

ADAMTS6: ADAM metallopeptidase with thrombospondin type 1 motif, 6

AJ: adherent junction

ANOVA: analysis of variance

BBB: blood brain barrier

BCAA: branched amino acid

BMVEC: brain microvascular endothelial cells

BSA: bovine serum albumin

CM: conditioned medium

CNS: central nerve system

DMEM: Dulbecco´s modified eagle medium

ECGS: endothelial cell growth supplements

EGF: epidermal growth factor

EM: epithelial cell growth medium

EMT: epithelial to mesenchymal transition

ESM1: endothelial cell-specific molecule 1 / endocan

FC: fold change

FCS: fetal calf serum

FGF: fibroblast growth factor

FDR: false discovery rate

FOXS1: forkhead box S1

 doi:10.20944/preprints202212.0342.v1

GBM: glioblastoma

GJ: gap junction

GPR183: G protein-coupled receptor 183

HBVP: human brain microvascular pericytes

HRP: horseradish peroxidase

IGF-1: insulin-like growth factor 1

KEGG: Kyoto Encyclopedia of Genes and Genomes

mTORC1: mammalian target of rapamycin complex 1

NOX4: NADPH oxidase 4

NVU: neurovascular unit

o/n: over night

OxPhos: oxidative phosphorylation

PBMVEC: porcine brain microvascular endothelial cells

PCA: principal component analysis

PGS: pericyte growth supplement

PLL: poly-L-lysine

PM: pericyte medium

PMET: plasma membrane electron transport

PPARGC1AC: peroxisome proliferator-activated receptor gamma, coactivator 1 alpha

PRR5: proline rich 5 like

P/S: penicillin/streptomycin

RT: room temperature

SLC46A3: solute carrier family 46, member 3

SD: standard deviation

SEM: standard error of the mean

SPOCK1: sparc/osteonectin, cwcv and kazal-like domains proteoglycan 1

SV-GA: SV40 large T-antigene immortalized astrocytic cells

TEER: transendothelial electric resistance

TGF-β: transforming growth factor beta

TJ: tight junction

VEGF: vascular endothelial growth factor

ZO: zonula occludens

References

1. Langen, U.H., S. Ayloo, and C. Gu, *Development and Cell Biology of the Blood-Brain Barrier.* Annu Rev Cell Dev Biol, 2019. **35**: p. 591-613.
2. Wu, C.X., et al., *Peritumoral edema shown by MRI predicts poor clinical outcome in glioblastoma.* World J Surg Oncol, 2015. **13**: p. 97.
3. Iorgulescu, J.B., et al., *Concurrent Dexamethasone Limits the Clinical Benefit of Immune Checkpoint Blockade in Glioblastoma.* Clin Cancer Res, 2021. **27**(1): p. 276-287.

4. Jackson, S., et al., *Blood-brain barrier pericyte importance in malignant gliomas: what we can learn from stroke and Alzheimer's disease.* Neuro Oncol, 2017. **19**(9): p. 1173-1182.
5. Nwadozi, E., M. Rudnicki, and T.L. Haas, *Metabolic Coordination of Pericyte Phenotypes: Therapeutic Implications.* Front Cell Dev Biol, 2020. **8**: p. 77.
6. Huang, S.F. and O.O. Ogunshola, *Metabolomic profiling provides new insights into blood-brain barrier regulation.* Neural Regen Res, 2021. **16**(9): p. 1786-1787.
7. Mader, L., et al., *Pericytes/vessel-associated mural cells (VAMCs) are the major source of key epithelial-mesenchymal transition (EMT) factors SLUG and TWIST in human glioma.* Oncotarget, 2018. **9**(35): p. 24041-24053.
8. Wirsik, N.M., et al., *TGF-beta activates pericytes via induction of the epithelial to mesenchymal transition protein SLUG in glioblastoma.* Neuropathol Appl Neurobiol, 2021.
9. Stander, M., et al., *Decorin gene transfer-mediated suppression of TGF-beta synthesis abrogates experimental malignant glioma growth in vivo.* Gene Ther, 1998. **5**(9): p. 1187-94.
10. Major, E.O., et al., *Establishment of a line of human fetal glial cells that supports JC virus multiplication.* Proc Natl Acad Sci U S A, 1985. **82**(4): p. 1257-61.
11. Mantwill, K., et al., *YB-1 dependent oncolytic adenovirus efficiently inhibits tumor growth of glioma cancer stem like cells.* Journal of translational medicine, 2013. **11**: p. 216.
12. Bartussek, C., U. Naumann, and M. Weller, *Accumulation of mutant p53(V143A) modulates the growth, clonogenicity, and radiochemosensitivity of malignant glioma cells independent of endogenous p53 status.* Exp Cell Res, 1999. **253**(2): p. 432-9.
13. Thomsen, L.B., A. Burkhart, and T. Moos, *A Triple Culture Model of the Blood-Brain Barrier Using Porcine Brain Endothelial cells, Astrocytes and Pericytes.* PLoS One, 2015. **10**(8): p. e0134765.
14. Paolinelli, R., et al., *Wnt activation of immortalized brain endothelial cells as a tool for generating a standardized model of the blood brain barrier in vitro.* PLoS One, 2013. **8**(8): p. e70233.
15. Czupalla, C.J., S. Liebner, and K. Devraj, *In vitro models of the blood-brain barrier.* Methods Mol Biol, 2014. **1135**: p. 415-37.
16. Srinivasan, B., et al., *TEER measurement techniques for in vitro barrier model systems.* J Lab Autom, 2015. **20**(2): p. 107-26.
17. Wolburg, H., S. Liebner, and A. Lippoldt, *Freeze-fracture studies of cerebral endothelial tight junctions.* Methods Mol Med, 2003. **89**: p. 51-66.
18. Schindelin, J., et al., *Fiji: an open-source platform for biological-image analysis.* Nature methods, 2012. **9**(7): p. 676-82.
19. Bus, C., et al., *Human Dopaminergic Neurons Lacking PINK1 Exhibit Disrupted Dopamine Metabolism Related to Vitamin B6 Co-Factors.* iScience, 2020. **23**(12): p. 101797.
20. Pang, Z., et al., *Using MetaboAnalyst 5.0 for LC-HRMS spectra processing, multi-omics integration and covariate adjustment of global metabolomics data.* Nat Protoc, 2022. **17**(8): p. 1735-1761.
21. Malinovskaya, N.A., et al., *Endothelial Progenitor Cells Physiology and Metabolic Plasticity in Brain Angiogenesis and Blood-Brain Barrier Modeling.* Front Physiol, 2016. **7**: p. 599.
22. Cantelmo, A.R., et al., *Inhibition of the Glycolytic Activator PFKFB3 in Endothelium Induces Tumor Vessel Normalization, Impairs Metastasis, and Improves Chemotherapy.* Cancer Cell, 2016. **30**(6): p. 968-985.
23. Ochs, K., et al., *Immature mesenchymal stem cell-like pericytes as mediators of immunosuppression in human malignant glioma.* Journal of neuroimmunology, 2013. **265**(1-2): p. 106-16.
24. Svensson, A., et al., *Endogenous brain pericytes are widely activated and contribute to mouse glioma microvasculature.* PloS one, 2015. **10**(4): p. e0123553.
25. Thanabalasundaram, G., et al., *Regulation of the blood-brain barrier integrity by pericytes via matrix metalloproteinases mediated activation of vascular endothelial growth factor in vitro.* Brain Res, 2010. **1347**: p. 1-10.
26. Patabendige, A. and N.J. Abbott, *Primary porcine brain microvessel endothelial cell isolation and culture.* Curr Protoc Neurosci, 2014. **69**: p. 3 27 1-17.
27. Gericke, B., et al., *A face-to-face comparison of claudin-5 transduced human brain endothelial (hCMEC/D3) cells with porcine brain endothelial cells as blood-brain barrier models for drug transport studies.* Fluids Barriers CNS, 2020. **17**(1): p. 53.
28. Thomsen, M.S., et al., *The blood-brain barrier studied in vitro across species.* PLoS One, 2021. **16**(3): p. e0236770.
29. Papetti, M., et al., *FGF-2 antagonizes the TGF-beta1-mediated induction of pericyte alpha-smooth muscle actin expression: a role for myf-5 and Smad-mediated signaling pathways.* Invest Ophthalmol Vis Sci, 2003. **44**(11): p. 4994-5005.
30. Thanabalasundaram, G., et al., *The impact of pericytes on the blood-brain barrier integrity depends critically on the pericyte differentiation stage.* Int J Biochem Cell Biol, 2011. **43**(9): p. 1284-93.
31. Atis, M., et al., *Targeting the blood-brain barrier disruption in hypertension by ALK5/TGF-Beta type I receptor inhibitor SB-431542 and dynamin inhibitor dynasore.* Brain Res, 2022. **1794**: p. 148071.
32. Gong, L., et al., *TGF-beta links glycolysis and immunosuppression in glioblastoma.* Histol Histopathol, 2021. **36**(11): p. 1111-1124.
33. Hattingen, E., et al., *Phospholipid metabolites in recurrent glioblastoma: in vivo markers detect different tumor phenotypes before and under antiangiogenic therapy.* PLoS One, 2013. **8**(3): p. e56439.
34. Herst, P.M. and M.V. Berridge, *Plasma membrane electron transport: a new target for cancer drug development.* Curr Mol Med, 2006. **6**(8): p. 895-904.
35. Gan, X., et al., *PRR5L degradation promotes mTORC2-mediated PKC-delta phosphorylation and cell migration downstream of Galpha12.* Nat Cell Biol, 2012. **14**(7): p. 686-96.
36. Nishimura, A., et al., *Detrimental role of pericyte Nox4 in the acute phase of brain ischemia.* J Cereb Blood Flow Metab, 2016. **36**(6): p. 1143-54.

 doi:10.20944/preprints202212.0342.v1

37. Underly, R.G., et al., *Pericytes as Inducers of Rapid, Matrix Metalloproteinase-9-Dependent Capillary Damage during Ischemia.* J Neurosci, 2017. **37**(1): p. 129-140.
38. Sanchis-Gomar, F., et al., *Mitochondrial biogenesis in health and disease. Molecular and therapeutic approaches.* Curr Pharm Des, 2014. **20**(35): p. 5619-33.
39. Liang, H. and W.F. Ward, *PGC-1alpha: a key regulator of energy metabolism.* Adv Physiol Educ, 2006. **30**(4): p. 145-51.
40. Zhenyukh, O., et al., *High concentration of branched-chain amino acids promotes oxidative stress, inflammation and migration of human peripheral blood mononuclear cells via mTORC1 activation.* Free Radic Biol Med, 2017. **104**: p. 165-177.
41. Ding, Y., et al., *DEPTOR Deficiency-Mediated mTORc1 Hyperactivation in Vascular Endothelial Cells Promotes Angiogenesis.* Cell Physiol Biochem, 2018. **46**(2): p. 520-531.
42. Banks, W.A., et al., *Healthy aging and the blood-brain barrier.* Nat Aging, 2021. **1**(3): p. 243-254.
43. Barnes, S., et al., *Omega-3 fatty acids are associated with blood-brain barrier integrity in a healthy aging population.* Brain Behav, 2021. **11**(8): p. e2273.
44. May, J.M. and Z.C. Qu, *Ascorbic acid efflux from human brain microvascular pericytes: role of re-uptake.* Biofactors, 2015. **41**(5): p. 330-8.
45. McMillin, M.A., et al., *TGFbeta1 exacerbates blood-brain barrier permeability in a mouse model of hepatic encephalopathy via upregulation of MMP9 and downregulation of claudin-5.* Lab Invest, 2015. **95**(8): p. 903-13.
46. Krizbai, I.A., et al., *Endothelial-mesenchymal transition of brain endothelial cells: possible role during metastatic extravasation.* PLoS One, 2015. **10**(3): p. e0123845.
47. Shen, W., et al., *Tyrosine phosphorylation of VE-cadherin and claudin-5 is associated with TGF-beta1-induced permeability of centrally derived vascular endothelium.* Eur J Cell Biol, 2011. **90**(4): p. 323-32.
48. Dohgu, S., et al., *Brain pericytes contribute to the induction and up-regulation of blood-brain barrier functions through transforming growth factor-beta production.* Brain Res, 2005. **1038**(2): p. 208-15.
49. Jones, B., *Targeted therapies: early vessel normalization improves glioblastoma outcomes.* Nat Rev Clin Oncol, 2014. **11**(1): p. 4.
50. Stylianopoulos, T. and R.K. Jain, *Combining two strategies to improve perfusion and drug delivery in solid tumors.* Proc Natl Acad Sci U S A, 2013. **110**(46): p. 18632-7.